Development of a Position Control Scheme for Rotating Sensor Unit Attached to In-pipe Robot

Hideki Wada[1], Masahiro Oya[2], and Katsuhiro Okumura[3]
[1]Shin-Nippon Nondestructive Inspection Co.,4-10-13 Ibori, Kokurakita-ku, Kitakyusyu-shi, Fukuoka, 803-8517 Japan
(Tel: 81-93-581-1256, Fax: 81-93-581-2232, E-mail: h-wada@shk-k.co.jp)
[2]Kyushu Institute of Technology, 1-1 Sensui-cho, Tobata-ku, Kitakyusyu-shi, Fukuoka, 804-8550 Japan
[3]Fukuoka Industrial Technology Center, Norimatu, Yahatanisi-ku, Kitakyusyu-shi, Fukuoka 807-0831 Japan

Abstract: In this paper, we propose a position control scheme for the rotation axis of a rotating ultrasonic sensor unit with a position adjustment mechanism. The control objective is that the position of the rotation axis can become equal to the center of a pipe. To realize the control objective, we provide a method to measure the vertical and horizontal position of the rotation axis. Using the measurements, we propose a position controller for the rotation axis. By carrying out experiments, we investigate the usefulness of the developed mechanism and the proposed position controller. As a result, it is shown that the proposed position control scheme has good performance.

Keywords: In-pipe Robot, Thickness measurement of the pipe, Ultrasonic sensor

1 INTRODUCTION

In the power generation plants, chemical plants and steel mills, the pipes may be deteriorated over time. Since these pipes have enormous length, it is a difficult task for human to inspect the deterioration state of the pipes [1]. Here, the deterioration state of the pipes means the decrease of the thickness of the pipes. To address the problem, we have developed inspection robots [2-8]. Those robots move on the outside of the pipes. Since most of such pipes are buried undergrounds or covered with the heat insulator, the high precision inspection can not be expected. For the reason, we have developed an in-pipe robot which can inspect the deterioration state from the inside of the pipes [9]. The robot has the inspection sensor unit in which ultrasonic sensors can be rotated in the circumferential direction of the pipe. However, there is a serious problem that the rotation axis in the inspection sensor unit may deviate from the center of the pipe while the in-pipe robot is moving inside the pipe. In such a case, the scanning speeds of the ultrasonic sensors are not constant and unknown. Then, the measurement precision of the thickness of the pipes may become worse.

To overcome this problem, we develop a new inspection sensor unit with a position adjustment mechanism for the rotation axis, and we propose a position control scheme. Namely, we provide a method to measure the vertical position and horizontal position of the rotation axis. Using the measurements, we propose a controller so that the position of the rotation axis can stay at the center of the pipe even if the in-pipe robot is moving inside the pipe.

2 OVERVIEW OF THE INSPECTION SYSTEM

Fig. 1 shows the overview of the in-pipe robot developed in [9]. The inspection sensor unit is attached to the front of the in-pipe robot (see the right hand side of Fig. 1). The inspection sensor unit has four inspection arms, and one ultrasonic sensor is attached on the top of the each inspection arm. Fig. 2 shows the details of the inspection arm. The inspection arm is composed of the holder part and the sliding part. Using a ball screw and a motor, the sliding

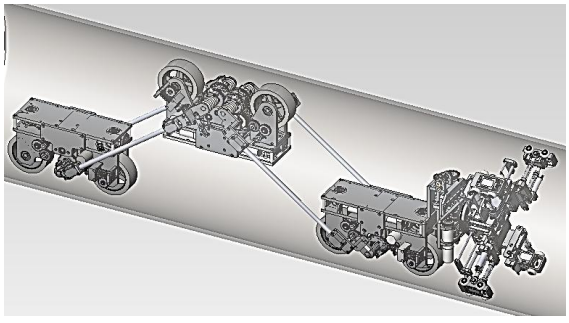

Fig. 1 Overview of the in-pipe robot.

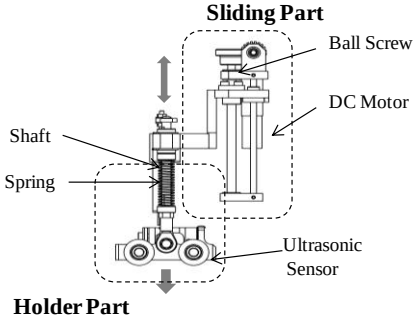

Fig. 2 Inspection arm.

part can move the holder part. There is a spring in the holder part. The ultrasonic sensor is pushed on the inner surface by the spring force. Moving the in-pipe robot and rotating the inspection arms, the all pipe thickness can be measured.

Fig. 3 shows the schematic of the initial configuration of the inspection sensor unit. The symbols l_{si} ,i =1~4 are the spring strokes that are the distance from the rotation axis to the inner surface of the pipe. The symbol l_{sp} denotes the fixed stroke of the sliding part. In the initial configuration, the rotation axis corresponds to the center of the pipe. In this situation, all of the spring strokes l_{si} become same and the scanning speeds of the ultrasonic sensors become a known constant speed. Then, the high precision inspection can be expected. However, while the in-pipe robot is moving inside the pipe, the center of the in-pipe robot may move due to the influence of disturbances. In that case, the rotation axis of the inspection arms deviates from the center of the pipe. Fig. 4 shows the displacements x_p, y_p of the rotation axis. The scanning speeds of the ultrasonic sensors on the inner surface are not constant when the inspection arms are rotated. Furthermore, because of a lack of information of the position of the rotation axis, the accurate location of the ultrasonic sensor cannot be obtained. Due to the influence, the measurement precision of the thickness may become worse.

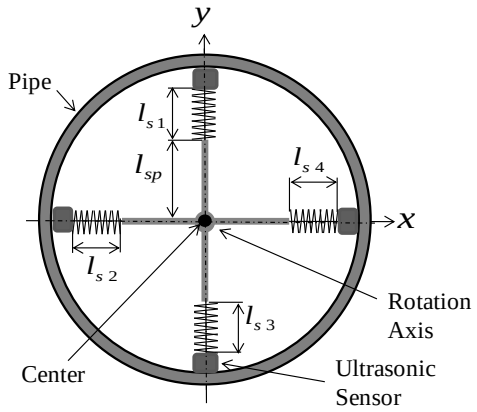

Fig. 3 Schematic of initial configuration.

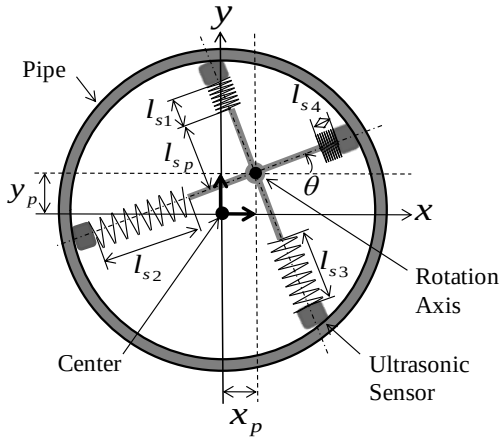

Fig. 4 Schematic in the presence of the deviation of the rotation axis.

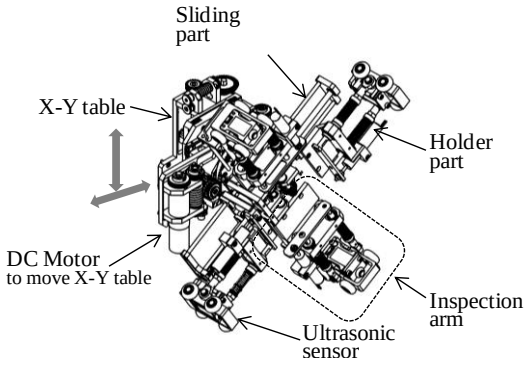

Fig. 5 Movable inspection unit.

3 MOVABLE INSPECTION SENSOR UNIT

To overcome the problem stated in the section 2, we develop an inspection sensor unit with a position adjustment mechanism for the rotation axis. Hereafter, the sensor unit is called the movable inspection unit. Fig. 5 shows the developed movable inspection unit. As shown in Fig. 5, the unit contains an adjustment mechanism (X-Y table) to move the rotation axis of the inspection arm. In order to make the position of the rotation axis be equal to the position of the center of the pipe, we require the displacement of the rotation axis from the center of the pipe.

3.1 Measurement of displacement of rotation axis

Fig. 6 shows the displacements x_p, y_p of the rotation axis. In Fig. 6, l_i ,i =1~4 are the distances from the rotation axis to the inner surface of the pipe. The symbol θ is the rotation angle of the inspection arms. In Fig.6, x_θ and y_θ can be written by

$$x_\theta = \frac{l_4 - l_2}{2}, \quad y_\vartheta = \frac{l_3 - l_1}{2} \tag{1}$$

Using the equation (1), we have the following

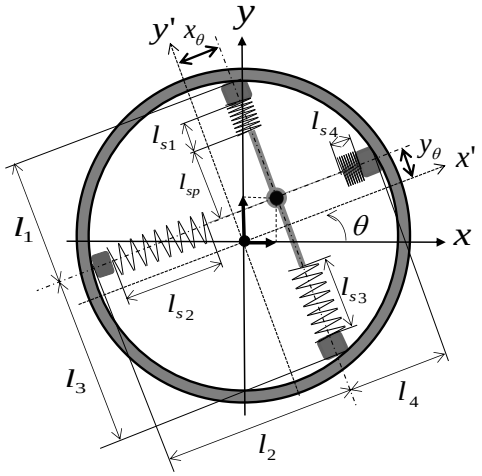

Fig. 6 The displacement of the rotation axis.

displacement of the rotation axis.

$$\begin{bmatrix} x_p \\ y_p \end{bmatrix} = \begin{bmatrix} \cos\theta & -\sin\theta \\ \sin\theta & \cos\theta \end{bmatrix} \begin{bmatrix} x_\theta \\ y_\theta \end{bmatrix} = \begin{bmatrix} \cos\theta & -\sin\theta \\ \sin\theta & \cos\theta \end{bmatrix} \begin{bmatrix} \frac{l_4 - l_2}{2} \\ \frac{l_3 - l_1}{2} \end{bmatrix} \quad (2)$$

Since the initial length of l_{sp} is fixed, the displacement of the rotation axis can be rewritten as

$$\begin{bmatrix} x_p \\ y_p \end{bmatrix} = \begin{bmatrix} \cos\theta & -\sin\theta \\ \sin\theta & \cos\theta \end{bmatrix} \begin{bmatrix} \frac{l_{s4} - l_{s2}}{2} \\ \frac{l_{s3} - l_{s1}}{2} \end{bmatrix} \quad (3)$$

In the developed movable inspection unite, the rotation angle θ and the spring strokes l_{si} can be measured. Using the measurements, we can calculate the displacements x_p, y_p of the rotation axis.

3.2 Position control of the rotation axis

To simplify the construction of the position controller, we derive a simplified model of the movable inspection sensor unit. Fig.7 shows the block diagram of the simplified model I for x axis direction. We can obtain the similar block diagram for y axis direction. In Fig. 7, u_x denotes the input signal (duty ratio ± 100%) added to DC motor to move the X-Y table, T_x is the equivalent time constant and K_x is the equivalent gain from the input to velocity $\dot{x}_p$ .The symbol d_x denotes the disturbance corresponding to the reaction force of springs which are attached to the holder parts in the inspection arms (see Fig.2). It is assumed that the equivalent time constant T_x is very short. Then, we propose a simplified model II shown in Fig. 8. Based on simplified model II, the following position controller is developed.

$$\begin{bmatrix} u_x \\ u_y \end{bmatrix} = -100 \begin{bmatrix} \operatorname{sgn} x_p \\ \operatorname{sgn} y_p \end{bmatrix} \quad (4)$$

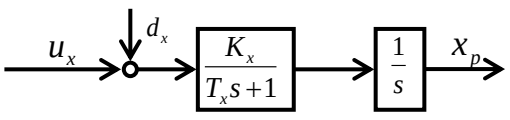

Fig. 7 Simplified model I.

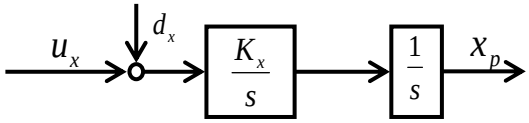

Fig. 8 Simplified model II.

4 EXAMINATIONS

4.1 Measurement of the displacement x_p, y_p

Fig. 9 shows the test equipment for the experiment of the position measurement of the rotation axis. The test equipment consists of ϕ350 acrylics pipe, the movable inspection sensor unit and the support base to fix the movable inspection sensor unit. The support base has the mechanism that the whole movable inspection sensor unit can be moved to top and bottom (y_M), right and left (x_M) by the handle operation. Using the mechanism, the position of the rotation axis can be moved from the center of pipe. The accurate displacements x_M, y_M of the rotation axis of the movable inspection unit is measured by using high precision encoders.

In the initial configuration, the position of the rotation axis and the center of the pipe are the same, and the rotation angle θ was fixed to be a certain angle. Then, the rotation axis is moved by using the handle attached to the support base, and the displacements x_p and y_p of the rotation axis are measured based on the equation (3).

The results of measurements of the displacements are shown in Figs 10-13. In Figs. 10 and 12, the horizontal axis denotes the accurate displacement x_M of the rotation axis which is moved by the handle operation. The accurate displacement y_M is fixed as $y_M = 0$. The vertical axis denotes the displacements x_p and y_p. In Figs. 11 and 13, the horizontal axis denotes the accurate displacement y_M of the rotation axis. The accurate displacement x_M is fixed as $x_M = 0$. The vertical axis denotes the displacement x_p and y_p.

As shown in Figs. 10-13, x_p and y_p are mostly same with the accurate displacements x_M and y_M. However, there exit small errors between the measurement displacements x_p, y_p and the accurate displacements x_M, y_M due to the low rigidity of the used acrylic pipe and the effect of gravity.

4.2 Position control position of the rotation axis

As with the measurement experiments of the displacement of the rotation axis, the test equipment shown

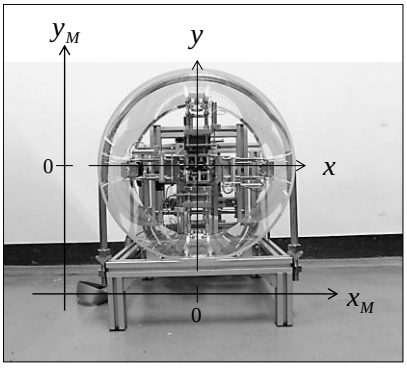

Fig. 9 The test equipment.

in Fig.9 is used in the position control experiments. In the initial configuration, the position of the rotation axis and the center of the pipe are the same, and the rotation angle θ was fixed to be zero. Next, the rotation axis is moved by the handle operation, and the inspection arms are rotated repeatedly within ±90[deg]. Then, the position control (4) is carried out.

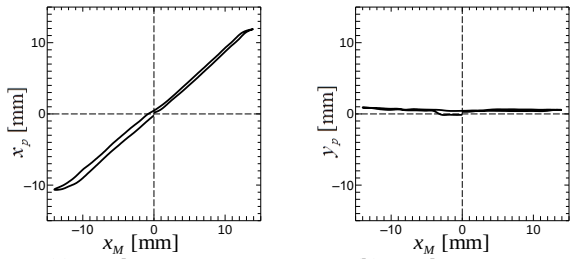

(a) Displacement x_p (b) Displacement y_p

Fig. 10 Displacement of the variation of x_M ($\theta = 0$).

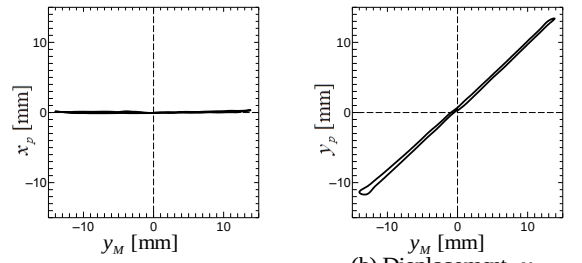

(a) Displacement x_p (b) Displacement y_p

Fig. 11 Displacement of the variation of y_M ($\theta = 0$).

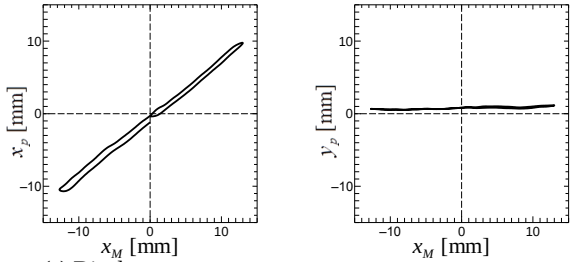

(a) Displacement x_p (b) Displacement y_p

Fig. 12 Displacement of the variation of x_M ($\theta = 30$).

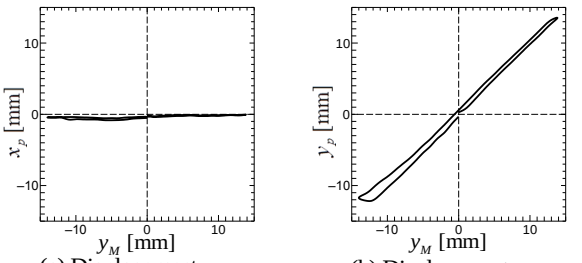

(a) Displacement x_p (b) Displacement y_p

Fig. 13 Displacement of the variation of y_M ($\theta = 30$).

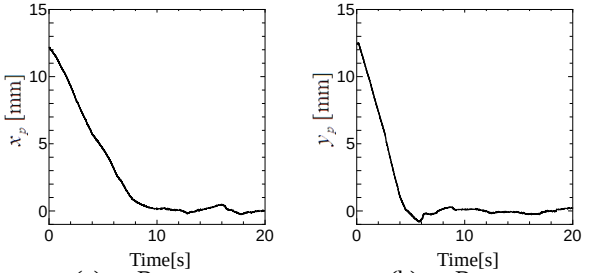

(a) x_p Response (b) y_p Response

Fig.14 Responses of the rotation axis.

Fig. 14 shows the responses of the displacements of the rotation axis. As shown in Fig. 14, the displacements x_p, y_p of the rotation axis converge to zero. Because of the effect of gravity, the convergence time of y_p becomes more quickly than that of x_p.

5 CONCLUSION

We develop an adjustment mechanism for the position of the rotation axis, and we propose the simple position controller for the adjustment mechanism. Carrying out experiments, it has been shown that the proposed position controller is very useful.

REFERENCES

[1] Y. Imagawa, H. Wada, Y. Wakibe, et al, Ultrasonic guided wave testing system for piping, Proc. of the ASME Pressure Vessels and Piping Conference, July 26-30, Prague Czech Republic, (in CD-ROM), (2009).

[2] T. Fukuda, H. Hosokai, and M. Otsuka, Autonomous pipeline inspection and maintenance robot with inch worm mobile mechanism, *Proc. of IEEE Int. Conf. on Robotics and Automation*, pp. 539-544, (1987).

[3] H. T. Roman and B. A. Pellegrino, "Pipe crawling inspection robot, An overview," *IEEE Trans. on Energy Conversion*, vol. 8 no. 3, pp. 576-583, (1993).

[4] H. B. Kuntze and H. Haffner, "Experiences with the development of a robot for smart multisensoric pipe inspection," *Proc. of IEEE Int. Conf. on Robotics and Automation*, pp. 1773-1778, (1998).

[5] S. G. Roh, S. M. Ryew, J. H. Yang, and H. R. Choi, Actively steerable in-pipe inspection robots for undergroung urban gas pipelines, *Proc. of IEEE Int. Conf. on Robotics and Automation*, pp. 761-766, (2001).

[6] M. Horodinca, I. Doroftei and E. Mignon : A Simple Architecture for In-Pipe Inspection Robots, Proceedings of the 2002 International Colloquium on Mobile and Autonomous Systems, pp.1-4, (2002).

[7] K. Suzumori, S. Wakimoto, and M. Takata, A miniature inspection robot negotiating pipes of widely varying diameter, *Proc. of IEEE Int. Conf. on Robotics and Automation*, pp. 2735-2740, (2003).

[8] H. Wada. (2010), Robotized for Nondestructive Testing (in Japanese), Proc. of The Japanese Society for Non-Destructive Inspection March 4-5, Tokyo, Japan, pp.17-20, (2010)

[9] k. Okumura, Y. Wtanabe, M. Oya, et al., Development of Inspection Robot Mechanism for Piping (in Japanese), Proceedings of Annual Conference of the Robotics Society of Japan, September 13-15, Chiba, Japan, (in CD-ROM), (2007).